Despeckling algorithm for reducing speckle noise in images generated from active sensors

H. Choi and J. Jeong✉

Synthetic aperture radar (SAR) images can be utilised in various fields because they are not affected by the time of day or weather conditions. However, in the process of employing active sensors to obtain a SAR image, speckle noise is generated in the image. Speckle noise degrades the ability of computer vision to observe the Earth. To improve imaging performance, an algorithm for removing speckle noise is necessary. For this purpose, the authors propose a speckle-noise removal algorithm. A speckle reducing anisotropic diffusion filter is employed as a pre-processing filter, in which multiplicative speckle noise can be converted into additive noise using a logarithmic transformation. To remove the additive noise, they use a weighted guided image filter. Experimental results indicate that the proposed method exhibits improved speckle noise suppression and edge preservation results compared with those of existing methods.

Introduction: An active sensor in aircraft, satellites, and spacecraft can acquire synthetic aperture radar (SAR) images [1]. Through SAR images, a ground target can be recognised without considering conditions such as the time of the day or weather conditions. Therefore, SAR images can be employed using active sensors in various fields, such as weather forecasting, agriculture, atmospheric studies, and military applications. Meanwhile, technologies related to SAR images have also been developed. Active sensors transmit electromagnetic echoes to targets and then construct 2D images by receiving the echoes from the target [1]. However, speckle noise appears in the SAR images because of the coherent interference of the reflected echoes [2]. Unlike other types of noise that are exhibited in other sensors, speckle noise demonstrates the characteristics of multiplicativity, a granular pattern, and Rayleigh distribution [3]. Speckle noise degrades image classification, recognition, feature extraction, and object detection because of the resulting low resolution. Therefore, a speckle noise removal method is a necessary technique for enhancing computer vision

To achieve this objective, a number of studies attempting to remove speckle noise without incurring a loss of edge information have been performed. Swamy and Vani [4] proposed an algorithm involving an improved threshold method in the curvelet domain for reducing speckle noise from SAR images. To adjust the adaptive spatiality of the regularisation parameter in non-local functions and suppress speckle noise from SAR images, Ma *et al.* [5] employed the local homogeneity index in the Lee filtering method [6]. Aubert and Aujol [7] proposed a speckle noise method based on the framework of the maximum a posteriori probability. Qiu *et al.* [8] attempted speckle noise suppression in SAR images by utilising the local mean and standard deviation. Despite these efforts, conventional algorithms exhibit low speckle noise suppression and edge conservation performance.

As mentioned above, to solve these two major problems, we utilise the statistical characteristics of the speckle noise and two filtering methods. As the speckle reducing anisotropic diffusion (SRAD) filter [9] has the instantaneous coefficient of variation (ICOV) to distinguish flat and edge areas in the speckled images, the SRAD filter is employed as a pre-processing filter. A logarithmic transformation is performed on the remaining speckle noise in the resultant image to change the multiplicative noise into additive noise. To reduce the additive noise of the image, a weighted guided image filter (WGIF) [10] is employed as a post-processing filter. Noise-free images are then obtained through an exponential transformation.

This paper is organised as follows. Section 2 introduces the SRAD filter, logarithmic transformation, and WGIF. In Section 3, we evaluate the experimental results of the conventional despeckling methods and the proposed algorithm. Section 4 concludes this Letter.

Proposed method: Initially, the proposed algorithm applies the SRAD filtering method, leading to immediate removal of speckle-noise that exhibits characteristics of multiplicative noise in the SAR images. This filtering technique uses a pre-processing filter that changes the multiplicative noise into additive noise by performing a logarithmic transformation. Next, the WGIF method is employed as it can reduce the additive noise in the image by using a post-processing filter. Thus, a combination of these two methods leads to the application of an exponential transformation, and finally, a noise-free image is captured.

An anisotropic diffusion (AD) filter shows excellent additive noise suppression and edge conservation abilities [9]. However, the AD filter does not suit speckle noise suppression because speckle noise has a different property from that of additive noise. The SRAD filtering technique was derived from the AD filter for direct application to images, including those with speckle noise [9].

The SRAD filtering technique uses a partial differential equation (PDE) to suppress the speckle noise from the SAR images. The PDE of the SRAD filtering method is as follows:

$$\begin{cases} \dfrac{\partial I(x, y; t)}{\partial t} = \operatorname{div}\left[c(q)\nabla I(x, y; t)\right] \\ I(x,\ y; 0) = I_0(x,\ y),\ \left(\dfrac{\partial I(x, y; t)}{\partial \boldsymbol{n}}\right)\Big|_{\partial\Omega} = 0 \end{cases} \tag{1}$$

where $I_0(x,\ y)$ has a finite power and no zero values over image support Ω, $I(x, y; t)$ denotes the output image, $\partial\Omega$ represents the border of Ω, and $\boldsymbol{n}$ denotes the outer normal of $\partial\Omega$.

From (1), diffusion coefficient (q) is used to characterise the diffusion scale of the SRAD filter. Parameter (q) is defined as

$$c(q) = \frac{1}{1 + \left[f^2(x, y, ; t) - f_0^2(t)\right]/T} \tag{2}$$

Here, $f_0(t)$ and T are the coefficient of variation over a flat region at some time t and threshold of the diffusion coefficient, respectively. Function $f(x, y; t)$ represents the ICOV, which can be calculated by employing (3)

$$q(x, y; t) = \sqrt{\frac{\left(\frac{1}{2}\right)\left(\frac{\nabla I}{I}\right)^2 - \left(\frac{1}{4^2}\right)\left(\frac{\nabla^2 I}{I}\right)^2}{\left[1 + \left(\frac{1}{4}\right)\left(\frac{\nabla^2 I}{I}\right)\right]^2}} \tag{3}$$

where ∇ is the gradient operator and ∇^2 is the Laplace operator. From (2), the value of $c(q)$ approaches zero when $f^2(x, y, ; t) - f_0^2(t)$ is greater than the value of T. From this process, the diffusion process is halted, the case of the reverse, the diffusion process is continued. The value of T is calculated as

$$T = f_0^2(t) \cdot \left(1 + f_0^2(t)\right) \tag{4}$$

Here, $f_0(t) = \dfrac{\sqrt{\operatorname{var}[z(t)]}}{\operatorname{mean}[z(t)]}$, and mean$[z(t)]$ and var$[z(t)]$ are the mean and variance of the flat areas at time t, respectively. Since the ICOV of the SRAD filter can distinguish between the edge regions and flat areas in the speckled images without a log-compression, in the proposed algorithm, it can be employed as a pre-processing filter [9].

The WGIF is used to treat the additive noise [10, 11]. To suppress the speckle noise from the resulting image using the SRAD filter, the speckle noise is converted into additive noise through the application of a logarithmic transformation [12]. The speckle noise is represented as

$$F(x, y) = S(x, y) \times M(x, y) \tag{5}$$

where $F(x, y)$ is the speckle noise image, $S(x, y)$ is the unknown original signal, and $M(x,\ y)$ is the multiplicative noise. The multiplicative noise can be converted into additive noise with the employment of the logarithmic transformation (6)

$$\begin{aligned} \operatorname{Log}\left(F(x, y)\right) &= \log\left(S(x, y)\right) + \log\left(M(x, y)\right) \\ &= Z(x, y) + e(x, y) \end{aligned} \tag{6}$$

where $Z(x, y) = \log\left(S(x, y)\right)$, [0, 1] and $e(x, y) = \log\left(M(x, y)\right)$.

The guided image filter (GIF) has excellent additive noise suppression performance [11]. As the value of the regularisation parameter is fixed in the GIF, a low preservation ability is demonstrated around the edge regions. Therefore, the GIF exhibits artefacts near the edge areas. To address this problem, in the WGIF, an edge-aware weighting method is applied to the GIF (7). The edge-aware weighting technique is as follows:

$$\Gamma_G\left((x, y)'\right) = \frac{1}{N}\sum_{k=1}^{N} \frac{\sigma_{G,1}^2\left((x, y)'\right) + \varepsilon}{\sigma_{G,1}^2\left((x, y)\right) + \varepsilon} \tag{7}$$

Here, G is a guidance image, $\sigma^2_{G,1}((x,y)')$ is the variance of the guidance image in a 3 × 3 window, $(x,y)'$ is the centre pixel of the square window, and ε is a small constant to prevent the denominator from going to zero. The value of ε is represented by $(0.001 \times L)^2$, where L denotes the dynamic range of the input image. The value of the edge-aware weight $\Gamma_G((x,y)')$ represents the characterisation of the flat areas or edge regions in the image. A value of $\Gamma_G((x,y)') > 1$ indicates that $(x,y)'$ is located in the edge areas; however, a value <1 occurs when $(x,y)'$ is located in the flat areas. To suppress the additive noise and maintain the areas near the edges, the edge-aware weighting technique [10] is applied to the GIF cost function (8)

$$E = \sum_{(x,y)\in\Omega_r(x,y)'} \left[\left(a_{(x,y)'} G(x,y) + b_{(x,y)'} - X(x,y) \right)^2 + \frac{\lambda}{\Gamma_G((x,y)')} a^2_{(x,y)'} \right] \tag{8}$$

where Ω_r is a square window centred at pixel (x,y) of a mask size r. The values of $a_{(x,y)'}$ and $b_{(x,y)'}$ are calculated as

$$a_{(x,y)'} = \frac{\mu_{G\odot X,r}((x,y)') - \mu_{G,r}((x,y)')\mu_{X,r}((x,y)')}{\sigma^2_{G,r}((x,y)') + \frac{\lambda}{\Gamma_G((x,y)')}} \tag{9}$$

$$b_{(x,y)'} = \mu_{X,r}((x,y)') - a_{(x,y)'}\mu_{G,r}((x,y)') \tag{10}$$

where Θ is the element-by-element product of two matrices, and $\mu_{G\odot X,r(x,y)'}$, $\mu_{G,r}((x,y)')$, and $\mu_{X,r}((x,y)')$ represent the average values of $G\Theta X$, G, and X, respectively.

Fig. 1 *Four standard test images*
a Cameraman
b Hill
c Lena
d Peppers

Table 1: Optimal values of parameters used for standard images

	Cameraman	Hill	Lena	Peppers
SRAD	time step = 0.01	time step = 0.01	time step = 0.01	time step = 0.01
	exponential decay rate = 1	exponential decay rate = 1	exponential decay rate = 1	exponential decay rate = 1
	number of iterations = 150	number of iterations = 115	number of iterations = 80	number of iterations = 130
WGIF	mask = 3×3	mask = 3×3	mask = 3×3	mask = 3×3
	Eps = 0.01	Eps = 0.01	Eps = 0.01	Eps = 0.01

The final value $\hat{Z}(x,y)$ is calculated as follows:

$$\hat{Z}(x,y) = \bar{a}_{(x,y)}G(x,y) + \bar{b}_{(x,y)} \tag{11}$$

Here, $\bar{a}_{(x,y)}$ and $\bar{b}_{(x,y)}$ are the average values of $a_{(x,y)'}$ and $b_{(x,y)'}$ in the window.

Experimental results: To assess the speckle noise suppression and edge conservation performances of the proposed technique, experiments were performed using four standard images, namely, Cameraman (256 × 256), Hill (512 × 512), Lena (512 × 512), and Peppers (256 × 256) (Fig. 1). Speckle noise with a variance of 0.04 was added to the four standard images. Table 1 denotes the optimal environmental conditions for four standard images. We used MATLAB R2018b (MathWorks, Natick, Massachusetts) to perform experiments related to image processing in this study.

Table 2: PSNR [dB] values for different despeckling methods

	Cameraman	Hill	Lena	Peppers
Noisy	18.6551	19.7850	18.8416	18.7385
Guided	18.6551	19.7850	18.8416	18.7385
Forst	22.4114	24.6391	24.2903	23.4965
Bitonic	22.8493	25.4834	25.8835	22.9169
Lee	24.4348	27.5784	28.5478	26.6410
SRAD	26.7292	28.0143	29.6024	28.2691
SG method	26.5849	28.4198	29.7588	26.6410
Proposed	**26.9338**	**28.6960**	**30.2464**	**28.2090**

Table 3: SSIM values for different despeckling methods

	Cameraman	Hill	Lena	Peppers
Noisy	0.4170	0.3752	0.2870	0.3753
Guided	0.4170	0.3752	0.2870	0.3753
Forst	0.4763	0.5282	0.4549	0.5397
Bitonic	0.5675	0.6392	0.5995	0.6473
Lee	0.6732	0.6949	0.7264	0.7654
SRAD	0.7619	0.7156	0.7778	0.8142
SG method	0.7833	0.7414	0.8163	0.7654
Proposed	**0.7989**	**0.7573**	**0.8296**	**0.8369**

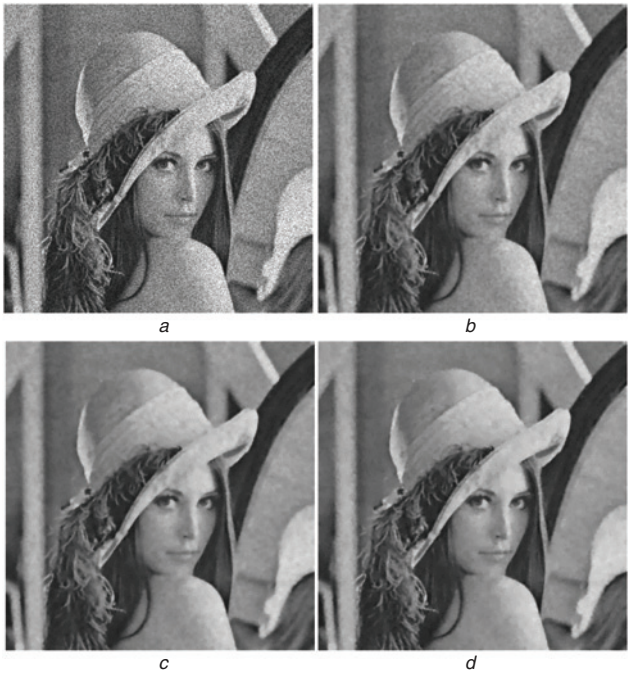

Fig. 2 *Filtered images for Lena contaminated by speckle noise*
a Noisy
b SRAD
c SG method
d Proposed

To evaluate the overall ability of speckle-noise suppression and edge conservation of the conventional and proposed methods, the following existing methods were considered: guided [13], frost [14], Lee [15], bitonic [16], SRAD [9], and SRAD-guided (SG) method [17]. To perform a quantitative comparison of the speckle noise elimination and edge conservation abilities of the conventional methods and

proposed algorithm, the peak signal-to-noise ratio (PSNR) and structural similarity (SSIM) indexes were adopted [11].

Tables 2 and 3 represent the PSNR and SSIM values of the conventional and proposed methods. Here, PSNR and SSIM values exhibiting the first-rank are presented in bold font for clarity. Tables 2 and 3 demonstrate that the proposed method performs better than the existing methods as shown by the PSNR and SSIM indexes. Fig. 2 shows the filtered images for the Lena image containing speckle noise. Although both the SG method and the proposed algorithm have a similar speckle noise suppression performance, the proposed method shows better speckle-noise reduction ability in the homogeneous regions. Fig. 3 presents the filtered Peppers image. As mentioned above, we can confirm that although the proposed method presents similar results to those of the SG method, the proposed algorithm exhibits better speckle noise suppression and edge preservation abilities than those of the SG technique.

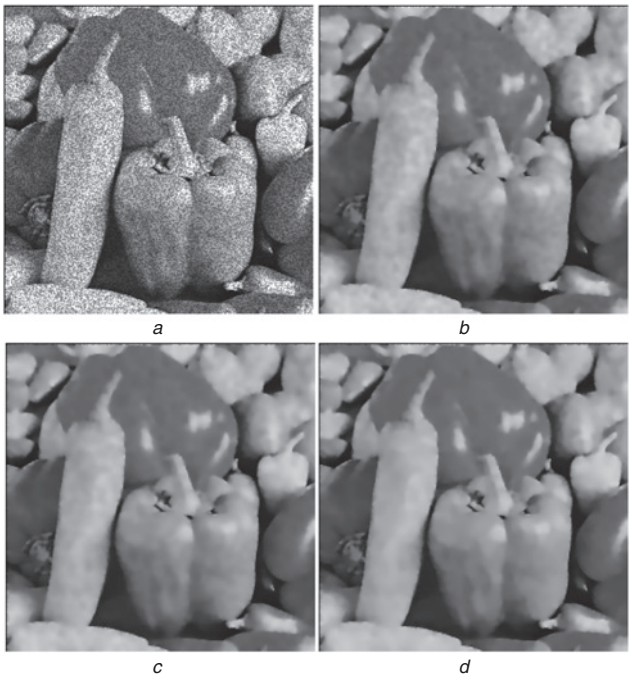

Fig. 3 *Filtered images for Peppers contaminated by speckle noise*

a Noisy
b SRAD
c SG method
d Proposed

Conclusion: We propose a novel despeckling algorithm using an SRAD filter, the statistical characteristics of speckle noise, and a WGIF to suppress speckle noise generated from active sensors of SAR images. The proposed method exhibits excellent despeckling performance in the flat areas and edge conservation near the edge regions. The results of the qualitative and quantitative analyses indicate that the proposed algorithm outperforms the conventional methods.

Acknowledgments: This work was supported by the research fund of the Signal Intelligence Research Center supervised by Defense Acquisition Program Administration and Agency for Defense Development of Korea.

Submitted: *09 March 2020* E-first: *22 June 2020*
doi: 10.1049/el.2020.0614
One or more of the Figures in this Letter are available in colour online.

H. Choi and J. Jeong (*Department of Electronics and Computer Engineering, Hanyang University, Seoul, Republic of Korea*)

✉ E-mail: jjeong@hanyang.ac.kr

References

1 Wang, K., Zhang, G., and Leung, H.: 'SAR target recognition based on cross-domain and cross-task transfer learning', *IEEE Access*, 2019, **7**, pp. 153391–153399
2 Wang, W., Xiang, D., Zhang, J., *et al*.: 'Superpixel-based classification using K distribution and spatial context for polarimetric SAR images', *Remote Sens.*, 2019, **11**, (4), pp. 1–20
3 Xie, H., Pierce, L.E., and Ulaby, F.T.: 'Statistical properties of logarithmically transformed speckle', *IEEE Trans. Geosci. Remote Sens.*, 2002, **40**, pp. 721–727
4 Swamy, P., and Vani, K.: 'A novel thresholding technique in the curvelet domain for improved speckle removal in SAR images', *Optik*, 2016, **127**, (2), pp. 634–637
5 Ma, X., Shen, H., Yuan, Q., *et al*.: 'Spatially adaptive nonlocal total variation for polSAR despeckling'. 2014 IEEE Geoscience and Remote Sensing Symp., Quebec City, Canada, July 2014, pp. 1670–1673
6 Lee, J., Grunes, M., and Grandi, G.D.: 'Polarimetric SAR speckle filtering and its implication for classification', *IEEE Trans. Geosci. Remote Sens.*, 1999, **37**, (5), pp. 2363–2373
7 Aubert, G., and Aujol, J.F.: 'A variational approach to remove multiplicative noise', *SIAM J. Appl. Math.*, 2008, **68**, (4), pp. 925–946
8 Qiu, F., Berglund, J., Jensen, J.R., *et al*.: 'Speckle noise reduction in SAR imagery using a local adaptive median filter', *GISci. Remote Sens.*, 2004, **41**, (3), pp. 244–266
9 Yu, Y., and Acton, S.T.: 'Speckle reducing anisotropic diffusion', *IEEE Trans. Image Process.*, 2002, **11**, (11), pp. 1260–1270
10 Li, L., Zheng, J., Zhu, Z., *et al*.: 'Weighted guided image filtering', *IEEE Trans. Image Process.*, 2014, **24**, (1), pp. 120–129
11 Zhang, J., Lin, G., Wu, L., *et al*.: 'Speckle filtering of medical ultrasonic images using wavelet and guided filter', *Ultrasonics*, 2016, **65**, pp. 177–193
12 Guo, Y., and Bai, Z.: 'A new denoising method of SAR images in curvelet domain'. 10th Int. Conf. on Control, Automation, Robotics and Vision, Hanoi, Vietnam, December 2008, pp. 17–20
13 He, K., Sun, J., and Tang, X.: 'Guided image filtering', *IEEE Trans. Pattern Anal. Mach. Intell.*, 2013, **35**, (6), pp. 1397–1409
14 Frost, V.S., Stiles, J.A., Shanmugan, K.S., *et al*.: 'A model for radar images and its application to adaptive digital filtering of multiplicative noise', *IEEE Trans. Pattern Anal. Mach. Intell.*, 1982, **PAMI-4**, (2), pp. 157–166
15 Lee, J.-S.: 'Refined filtering of image noise using local statistics', *Comput. Graph. Image Process.*, 1981, **15**, (4), pp. 380–389
16 Treece, G.: 'The bitonic filter: linear filtering in an edge-preserving morphological framework', *IEEE Trans. Image Process.*, 2016, **25**, (11), pp. 5199–5211
17 Choi, H., and Jeong, J.: 'Speckle noise reduction in ultrasound images using SRAD and guided filter'. Proc. Int. Workshop on Advanced Image Technology, Chiang Mai, Thailand, January 2018, pp. 1–4